

## CHAPTER 7

### TEST RESULTS

#### 7.1 General Remarks

Tests described in this section were carried out to predict ultimate load and moment factors with a purpose to provide validity check to theory.

Total of twenty four tests were performed. Specimens numbered as 1 to 12 formed the first set of testing programme, where  $Z$  ratio was kept as unity.  $mp$  values were 0.05, 0.07 and 0.2 for three groups. Each group contained four specimens. Four different eccentricity ratios were used in each group. The second set consisted of twelve specimens where  $Z$  ratios were kept as 1, 2 and 3 for three groups of specimens. Each group again contained four specimens. Four different eccentricity ratios were used in each group.

#### 7.2 Presentation of Test Data and Results

The test data of specimens used in experimental work are summarized in Table 6.3. The load-lateral deflection curves for twelve specimens are presented in Figs. 7.1, 7.2 and 7.3. Test results are produced in Table 8.1.

Crushing strength of concrete was taken as average of prism strength of each group. Tangent modulus of elasticity for concrete was determined separately for each prism with the help of its stress strain curve. The modular and the stress ratios were evaluated for the groups to prepare test data. The machine load was calibrated on standard proving ring certified by National Physical Research Laboratory, New Delhi. Test loads indicated were the collapse loads for specimens.

Plates No.1 through 24 show crack patterns at various stages of loading and at failure loads for the specimens tested. The photographs indicate clearly the width and breadth of cracks along with the trend of propagation of cracks and its history.

### 7.3 Behaviour Under Load and Mode of Failure

#### Load Deflection Curves

The load-deflection curves of beam column specimens represent an overall property useful for illustrating the behaviour under effect of variables.

The load-lateral deflections indicate two major stages of behaviour. First, the predominant elastic behaviour of specimens upto certain stage of loading

and second, the total inelastic behaviour thereafter. The lateral deflections become very large at the collapse. The first stage deflections can be approximated to straight lines. Magnitude of lateral deflection is governed by eccentricity ratio.

The gradual transition from elastic to non-elastic stage of behaviour was due to progressive yielding of the tension reinforcement along the corner of tension side. As the yielding progressed, the crushing of concrete started leading to ultimate failure of specimens.

#### Cracking Pattern and Mode of Failure

A study of formation and the development of cracks in a reinforced concrete member under load is essential and significant to predict behaviour and mode of failure.

Close look reveals that the cracks start at the extreme tension corner and propagate deep thereafter.

An observation through the crack pattern points out the probable location of neutral axis. A shift in its position is also demonstrated as the load progresses.

Increase in tension steel content, brings heavy

crack patterns. Large eccentricity ratios exhibit thin net of cracks, with wide and deep crack patterns.

More compression reinforcement reduces cracks on compression concrete. Yielding of tension steel in such cases is, however, accelerated, resulting into rapid crack propagation on tension faces.

Tension failure exhibits accurate predictions. Compression failure is also predicted well but the test loads tend to be on lower side of calculated loads. For large eccentricities, the specimens have exhibited strengths more than that predicted. The eccentricity ratios affect strength sensitively.

Three modes of failure observed are :

- (a) Yielding of tension steel followed by crushing concrete
- (b) Compression failure with no yielding of tension steel
- (c) Shear failure of brackets and subsequent miscellaneous local failures.

Specimens having largest eccentricity ratios are examples of tension failures. As the eccentricity reduces, a shift towards compression failure is observed. Further reduction in eccentricity ratio

should have resulted into ideal compression failure but owing to the fact that ultimate loads were large enough to cause the shear failure of brackets, the specimens have failed in brackets.

Local failures are attributed to crushing of concrete under the hinge devices and have not disturbed the measurement of ultimate loads as they have occurred at the later stage in some specimens.

Although the data are too few to justify the cause, it is realised that it has been helpful to observe the trend and behaviour along with the modes of failure. Further tests are undoubtedly necessary to enrich the efforts.

#### 7.4 Observations Regarding Crack Patterns and Mode of Failure

Details regarding crack patterns and modes of failure of individual specimen are described in the following.

Specimen 1, (MOP 1/5,  $e_y = 10.16$  cm,  $e_x = 3.81$  cm)

The crack pattern of the specimen after failure is shown in plate 1. Cracking started from tension corner and progressed along the specimen on adjacent

sides. Cracks are few in number. The maximum width of crack is at the tension corner. The exact mode of failure could not be judged.

Specimen 2, (MUP 1/5,  $e_y = 15.24$  cm,  $e_x = 3.81$  cm)

See plate 2. Crack pattern is spread on surface within the gauge length. Cracks have reached the adjacent corners. Vertical cracks were observed at bottom and top junction of column and bracket. The specimen failed due to local shearing of the bracket.

Specimen 3, (MUP 28/4,  $e_y = 20.32$  cm,  $e_x = 3.81$  cm)

Cracks are clearly shown in plate 3. All cracks were observed first at tension corner. They progressed towards compression corner. The widening of cracks indicated that the steel was yielding. Concrete crushed at the final stage of loading. The mode of failure was a tension failure.

Specimen 4, (MUP 28/4,  $e_y = 20.32$  cm,  $e_x = 0$  cm)

Plate 4 shows the crack pattern for this specimen.

Cracks were observed within the gauge length and were symmetrically proceeding on opposite faces.

It was a case of uniaxial loading. The tension failure, resulting into wide cracks on tension face followed by crushing of concrete on compression face, was observed.

Specimen 5, (MUP 2/5,  $e_y = 10.16$  cm,  $e_x = 3.81$  cm)

The specimen after failure with crack history is shown in plate 5.

Cracks were observed at tension corner. Some cracks have progressed upto middle of opposite faces. Local failure occurred due to crushing of concrete.

Specimen 6, (MUP 2/5,  $e_y = 15.24$  cm,  $e_x = 3.81$  cm)

Refer to plate 6 for photograph of this specimen. All cracks were observed within gauge length, progressing from tension corner. Cracks have propagated to opposite faces. Local failure occurred. Bracket failed in shear.

Specimen 7, (MUP 4/5,  $e_y = 20.32$  cm,  $e_x = 3.81$  cm)

Crack pattern on tension face is seen clearly in plate 7. Location and orientation of cracks are photographed. Crushing of concrete on compression face is observed.

Specimen 8, (MUP 4/5,  $e_y = 20.32$  cm,  $e_x = 0$  cm)

Crack pattern, location and orientation of crack lines are shown in plate 8. This is a case of uniaxial loading and it is clearly exhibited in its behaviour. Neutral axis is symmetrically located. It is a case of tension failure.

Specimen 9, (MUP 3/5,  $e_y = 5.08$  cm,  $e_x = 1.30$  cm)

Upto 20 tonnes, no crack was observed. It is a case of compression failure. No specific crack pattern is observed. See plate 9.

Specimen 10, (MUP 3/5,  $e_y = 10.16$  cm,  $e_x = 2.60$  cm)

Photograph is presented in plate 10. Crack pattern, location and orientation of crack patterns are observed. Few cracks are observed progressing from tension surface towards the adjacent corners. Crushing of concrete was marked clearly.

Specimen 11, (MUP 3/5,  $e_y = 20.32$  cm,  $e_x = 3.81$  cm)

See plate 11. Cracks have developed within the gauge length. Splitting of concrete is observed.. Compression failure is not clearly indicated.

Specimen 12, (MUP 3/5,  $e_y = 20.32$  cm,  $e_x = 0$  cm)

See plate 12. Large number of cracks is observed. Yielding of tension steel is clearly exhibited. Spalling of concrete ~~was~~ occurred at compression face due to crushing of concrete at middle of gauge length. This is a case of tension failure.

The first twelve specimens were tested under a pilot testing programme. Based on that performance, some modifications were done in subsequent testing programme to avoid local failure cases. The twelve specimens which follow had  $Z$  ratio as a variable.

Specimen 13, (S1 7/5,  $e_y = 20$  cm,  $e_x = 4$  cm)

Plate 13 shows details of crack patterns of this specimen. The observations were: failure within gauge length, crack started at 4.5 T. Spalling of concrete on compression face. Wide and deep crack at 7.0 T. Tension failure of specimen.

Specimen 14, (S1 4/5,  $e_y = 20$  cm,  $e_x = 0$  cm)

Crack started at 5.0 T. It is an uniaxial loading. It could be observed that the neutral axis

was progressing symmetrically. Tension failure was observed. Most of the cracks progressed up to half the width of long faces. Plate 14.

Specimen 15, (S1 4/5,  $e_y = 15$  cm,  $e_x = 4$  cm)

It failed in compression. Crushing of concrete was observed. Yielding started at later stage. Plate 15.

Specimen 16, (S1 7/5,  $e_y = 10$  cm,  $e_x = 4$  cm)

Failure of bracket was observed. In order to avoid such failure, it was decided to pursue the subsequent work at larger eccentricity in  $y$  direction. See plate 16.

Specimen 17, (S2 5/5,  $e_y = 25$  cm,  $e_x = 4$  cm)

Crushing reached at ultimate load. Inclination of neutral axis was clearly observed at various stages of loading. Specimen failed within gauge length. Lateral deformations were large. Few cracks are observed. Plate 17.

Specimen 18, (S2 5/5,  $e_y = 20$  cm,  $e_x = 0$  cm)

Splitting of concrete is seen. Neutral axis is parallel to width. Wide and large cracks are observed, but the number of cracks is less. Plate 18.

Specimen 19, (S2 5/5,  $e_y = 20$  cm,  $e_x = 4$  cm)

First crack observed at 5.5 T. near middle of gauge length. Widening of crack is evident. Tension failure is marked, yielding of reinforcement is clearly seen. Spalling of concrete subsequently at root of bracket. Plate 19.

Specimen 20, (S2 5/5,  $e_y = 15$  cm,  $e_x = 4$  cm)

Very few cracks are marked. Compression failure is observed. Crushing of concrete is seen. Failure within the gauge length. Plate 20.

Specimen 21, (S3 6/5,  $e_y = 25$  cm,  $e_x = 4$  cm)

Few cracks are observed. Tension failure case is marked. Spalling of concrete at extreme compression corner is seen at later stage of loading. Cracks at 4.5, 5, 6.0 T. are marked. Plate 21.

Specimen 22, (S3 6/5,  $e_y = 20$  cm,  $e_x = 0$  cm)

First crack at 6.5 T. Yielding of tension reinforcement is observed. Excessive yielding is clearly seen. Plate 22.

Specimen 23, (S3 6/5,  $e_y = 20$  cm,  $e_x = 4$  cm)

Tension failure case is observed. Spalling of concrete after surface cracking is seen at later stage. Number of cracks is less. Plate 23.

Specimen 24, (S3 6/5,  $e_y = 15$  cm,  $e_x = 4$  cm)

First crack was observed at 7.0 T. Yielding of tension steel and crushing of concrete are visible. Few cracks are observed. Plate 24.

#### 7.5 Test Results : Influence of Variables

The effect of variables on strength and behaviour of the beam column specimens tested are discussed in this section.

The variables considered were the amount of tension steel (specimens 1 to 12), Z ratio (specimens 13 to 24), the strength of concrete and the eccentricity ratios.

### Ratio of Compression to Tension Reinforcement

It is observed from the performance of specimens that the ratio of compression to tension reinforcement having values in the range of 1 to 3 does not contribute much to the strength of beam column specimens 13 to 24 can be studied in this respect. The beam columns 14, 18 and 22 have exhibited the ultimate loads of 7.0 T., 7.2 T. and 6.8 T. respectively. The corresponding ratios of  $Z$  were 1, 2 and 3. The results for specimens 15, 20 and 24 are 9.25 T., 11.0 T. and 10.2 T. respectively. The groups of specimens listed above had equal eccentricity ratios. Beam columns 13, 19 and 23 exhibit similar characteristics. It is, however, observed that specimens with  $Z = 2$ , demonstrated higher value of ultimate load.

### Amount of Tension Steel

The testing results of specimens with different amount of tension steel in the range of 1.45 to 3.0 percent, reveal that there is no effect of the reinforcement percentage on mode of failure. The study for this variable was deduced from specimens 1 to 12. Change in reinforcement content in these specimens have not changed the mode of failure, e.g. the specimens 3, 7 and 11 having different steel contents, have failed by

tension mode of failure. Specimens 4, 8 and 12 have also failed by same mode of failure.

### Strength of Concrete

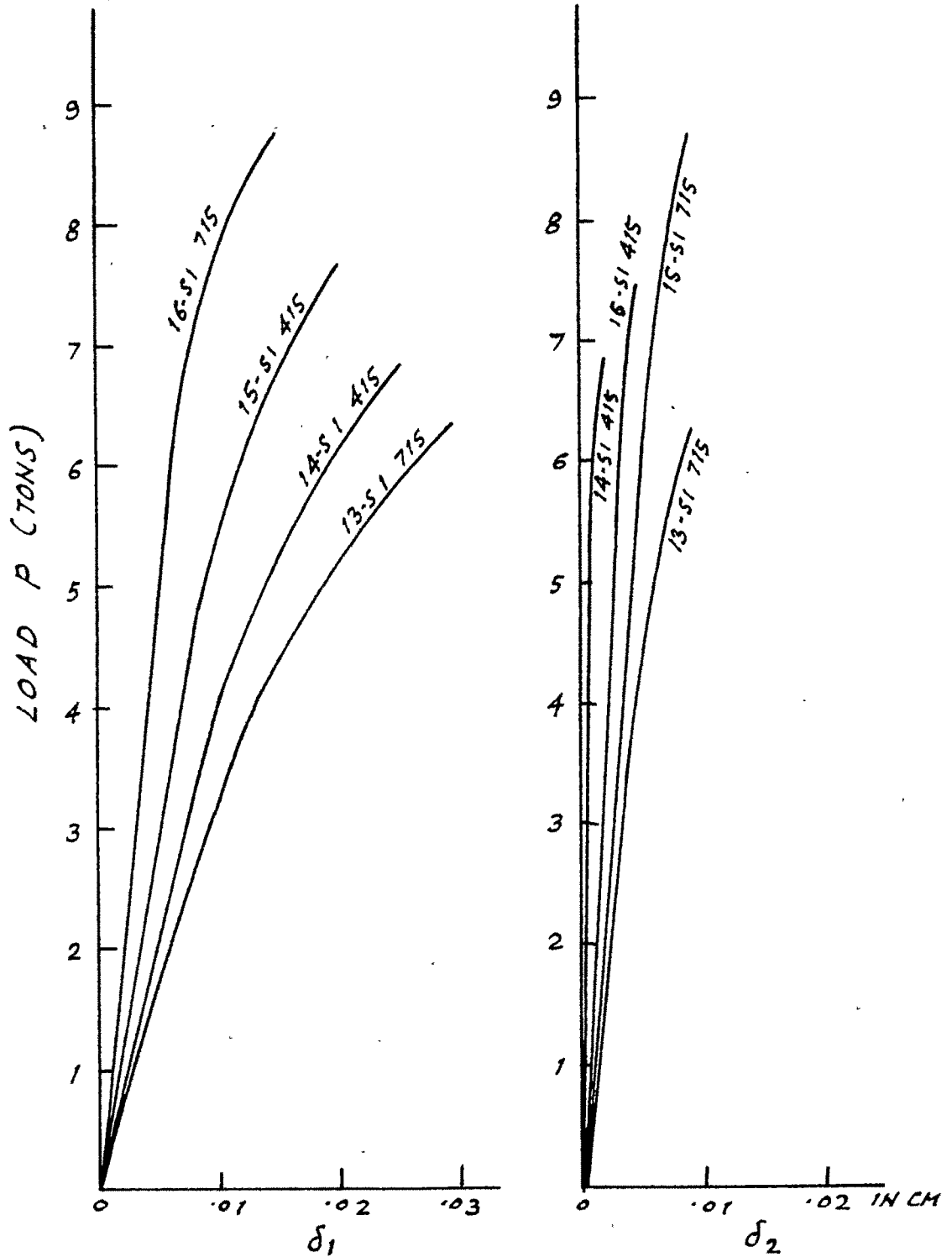
Ultimate load and moment capacities of specimens are observed to have improved in proportion to concrete strengths. Specimens 22, 14 and 18 having tested for equal eccentricity ratios have exhibited ultimate load capacities of 6.8 T., 7.0 T. and 7.2 T. for concrete strengths of 219.0, 227.0 and 239.2 kg/cm<sup>2</sup> respectively. Test specimens 24 and 20 exhibit similar characteristic.

### Eccentricity Ratios

The ultimate load and moment capacities are affected by the eccentricity ratio. Larger the eccentricity ratios, smaller are the capacities. This phenomena is exhibited by specimens 16, 15 and 14 where the ultimate load capacities were observed as 13.5 T., 9.25 T. and 7.0 T. respectively for eccentricity ratio of 10 cm, 15 cm and 20 cm in y-direction. Similar performance was observed in other specimens also.

## 7.6 Closure

The observations noted in the above paragraphs are based on test results of twenty four specimens only. Much more testing is required to make generalised observations. Hence, generality cannot be claimed through these observations. An effort, however, is made to add test results and observations to existing experimental data.

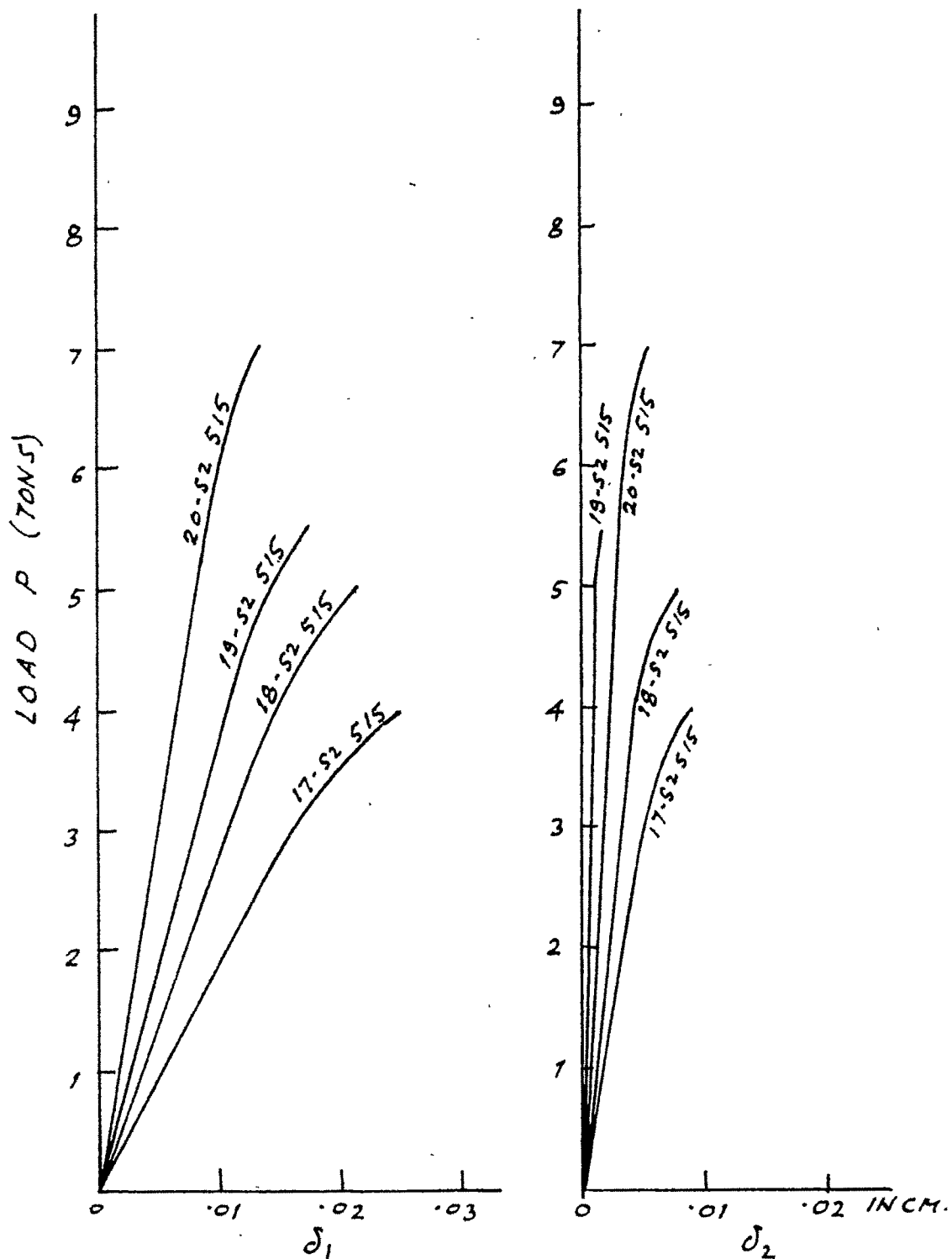


LOAD VS. LATERAL DEFLECTION

(A) ALONG Y-Y AXIS ( $\delta_1$ )

(B) ALONG X-X AXIS ( $\delta_2$ )

FIG. 7-1.

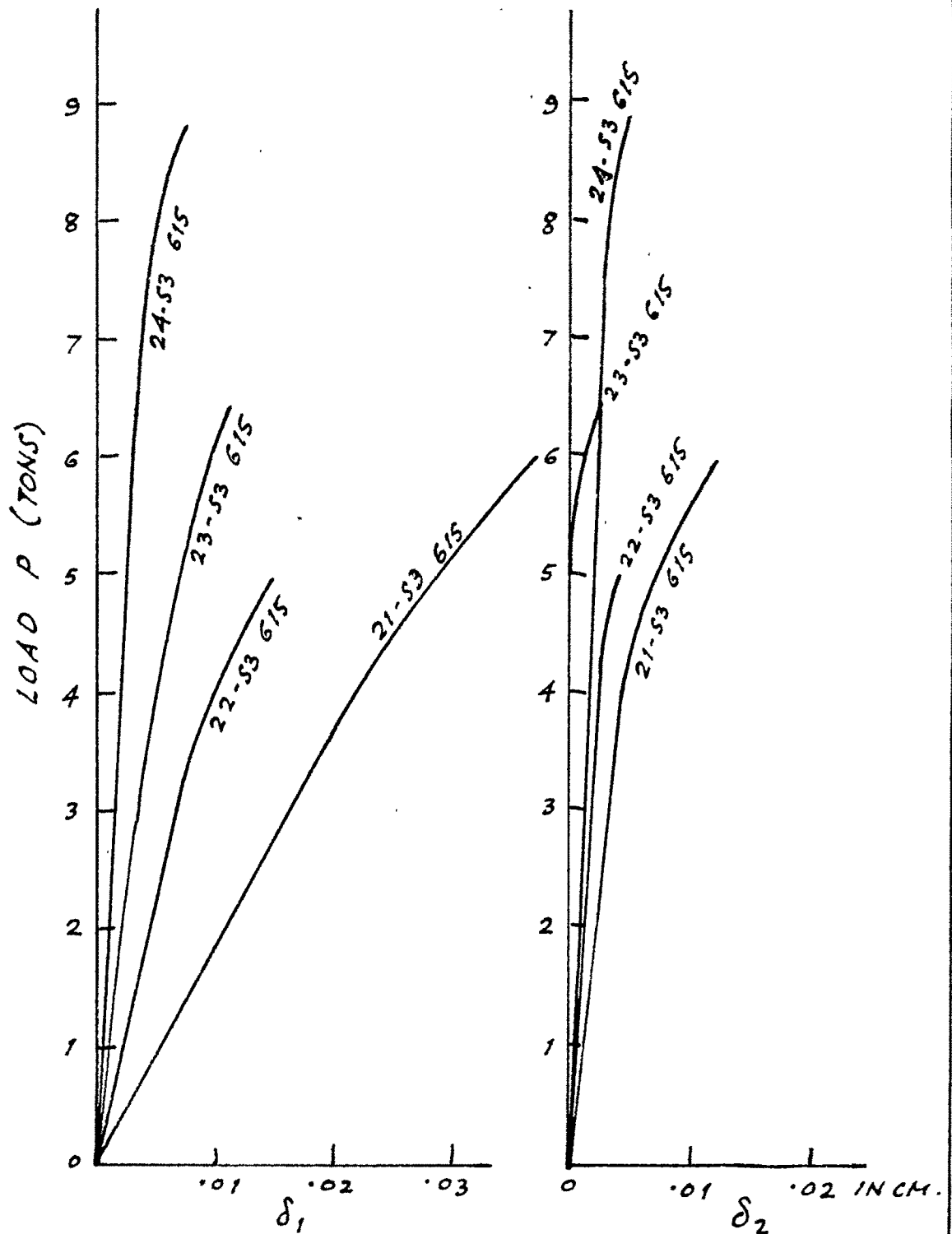


LOAD VS. LATERAL DEFLECTION

(A) ALONG Y-Y AXIS ( $\delta_1$ )

(B) ALONG X-X AXIS ( $\delta_2$ )

FIG. 7.2



LOAD VS. LATERAL DEFLECTION

(A) ALONG Y-Y AXIS ( $\delta_1$ )

(B) ALONG X-X AXIS ( $\delta_2$ )

FIG. 7-3